Mineralogical Magazine (2023), **87**, 218–224
doi:10.1180/mgm.2022.133

CAMBRIDGE UNIVERSITY PRESS

Article

Bounahasite, $Cu^{+}Cu^{2+}_{2}(OH)_{3}Cl_{2}$, a new mineral from the Bou Nahas Mine, Morocco

Inna Lykova[1]*, Ralph Rowe[1], Glenn Poirier[1], Henrik Friis[2] and Kate Helwig[3]

[1]Canadian Museum of Nature, PO Box 3443, Station "D", Ottawa, Ontario K1P 6P4, Canada; [2]Natural History Museum, University of Oslo, PO Box 1172, Blindern, 0318 Oslo, Norway; and [3]Canadian Conservation Institute, 1030 Innes Road, Ottawa, Ontario K1B 4S7, Canada

Abstract

The new mineral bounahasite, $Cu^{+}Cu^{2+}_{2}(OH)_{3}Cl_{2}$, was found in the oxidation zone of the Bou Nahas Mine, Morocco. It forms pseudo-hexagonal plates up to 3 × 30 × 40 μm in size combined in loose clusters with native copper and paratacamite. The mineral is green with vitreous lustre. The cleavage is parallel to {110}, perfect. D_{calc} is 3.90 g/cm^3. The infrared spectrum is reported. The composition (wt.%) is Cu_2O 23.26, CuO 51.72, Cl 23.36, H_2O 8.71, O = Cl_2 −5.27, total 101.78. The empirical formula calculated on the basis of 3 Cu atoms per formula unit is: $Cu^{+}Cu^{2+}_{2}(OH)_{2.97}Cl_{2.03}$. The mineral is monoclinic, $P2_1/n$, a = 8.5925(1), b = 6.4189(1), c = 10.4118(2) Å, β = 111.804(2)°, V = 533.17(2) Å^3 and Z = 4. The strongest reflections of the powder X-ray diffraction pattern [d,Å(I)(hkl)] are: 7.71(70)($\bar{1}$01), 5.34(22)(011), 3.856(100)(012, $\bar{2}$02), 2.673(36)(022), 2.665 (30)(103) and 2.350 (71)($\bar{1}$23, 301, $\bar{2}$14). The crystal structure, refined from single-crystal X-ray diffraction data (R_1 = 0.028), is based on two alternating sheets coplanar to (110): one consists of alternating edge-sharing $Cu^{2+}(OH)_6$ octahedra and two $Cu^{2+}(OH)_4Cl_2$ octahedra, whereas the other one is based on $Cu^{+}Cl_4$ tetrahedra forming edge-sharing $Cu^{+}_{2}Cl_6$ dimers.

Keywords: bounahasite, new mineral, crystal structure, supergene, Bou Nahas Mine, Morocco

(Received 26 July 2022; accepted 25 November 2022; Accepted Manuscript published online: 9 December 2022; Associate Editor: Owen Missen)

Introduction

Copper(II) hydroxychloride minerals are typical oxidation products of other copper minerals under arid conditions. This paper describes the first mixed-valency copper hydroxychloride mineral bounahasite, $Cu^{+}Cu^{2+}_{2}(OH)_{3}Cl_{2}$. Only two other minerals with both univalent and divalent copper cations are known – a rare secondary mineral paramelaconite $Cu^{+}_{2}Cu^{2+}_{2}O_3$ (O'Keeffe and Bovin, 1987) and a rare fumarolic mineral allochalcoselite $Cu^{+}Cu^{2+}_{5}PbO_2(SeO_3)_2Cl_5$ (Vergasova *et al.*, 2005; Krivovichev *et al.*, 2006).

Bounahasite was named after its type locality – Bou Nahas Mine, Morocco. Both the new mineral and the name (symbol Bnhs) have been approved by the Commission on New Minerals, Nomenclature and Classification of the International Mineralogical Association, proposal IMA2021-114 (Lykova *et al.*, 2022). The holotype has been deposited in the collection of the Canadian Museum of Nature, Ottawa, Canada. The catalogue number is CMNMC 89874. A part of the holotype used for structure determination has been kept at the Natural History Museum in Oslo under catalogue number KNR 44404.

Occurrence and general appearance

Bounahasite occurs at the Bou Nahas (Bou N'hass) Cu Mine, Oumjrane mining area, Anti-Atlas Mountains, Morocco. It is a supergene mineral found in the oxidation zone of hydrothermal polymetallic veins. The veins were formed along faults and fractures in Upper Ordovician marlstones, shales, sandstones and conglomerates during hydrothermal activity related to late Triassic volcanism. The main minerals of the polymetallic veins are pyrite, chalcopyrite, galena and baryte. The secondary supergene mineralisation developed later, probably between Jurassic and Neogene periods (Praszkier, 2015).

The new mineral forms very small pseudo-hexagonal plates up to 3 × 30 × 40 μm in size. The dominant form is pinacoid {110} with minor rhombic prism and another pinacoid. The crystals are combined into loose clusters (Figs 1–2) on native copper together in association with paratacamite.

Physical and optical properties

Bounahasite is green with pale green powder colour and vitreous lustre (Fig. 1). The cleavage is parallel to {110}, perfect. The fracture is uneven, stepped. The Mohs hardness could not be determined as the crystals are very small. The mineral is non-fluorescent under ultraviolet light. The density calculated using the empirical formula and unit-cell volume refined from the single-crystal X-ray diffraction data is 3.90 g/cm^3.

Bounahasite is optically biaxial, 2V (meas.) = 60(5)° (from a spindle-stage extinction curve). The refractive indices were not measured due to the lack of available high refractive index (>1.8) immersion fluids. The mean refractive index obtained from the Gladstone–Dale relationship (Mandarino, 1981) is 1.961.

*Author for correspondence: Inna Lykova, Email: ilykova@nature.ca
Cite this article: Lykova I., Rowe R., Poirier G., Friis H. and Helwig K. (2023) Bounahasite, $Cu^{+}Cu^{2+}_{2}(OH)_{3}Cl_{2}$, a new mineral from the Bou Nahas Mine, Morocco. *Mineralogical Magazine* **87**, 218–224. https://doi.org/10.1180/mgm.2022.133

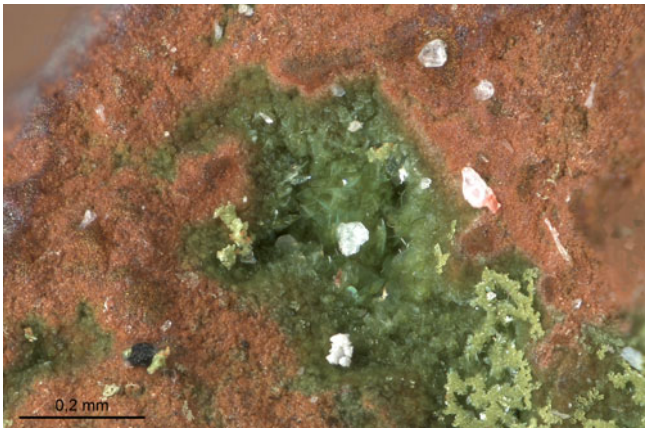

Fig. 1. Green platy crystals of bounahasite on native copper. FOV 1 mm. Specimen CMNMC 89874. Photo: François Génier.

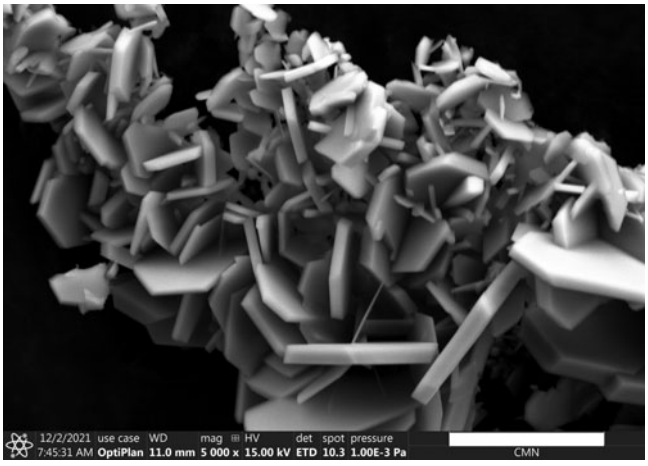

Fig. 2. Bounahasite crystals. Scanning electron microscopy image, scale bar = 10 μm.

Experimental methods

Electron microprobe analyses of bounahasite were obtained using a JEOL 8230 SuperProbe electron microscope equipped with five wavelength dispersive spectrometers (University of Ottawa – Canadian Museum of Nature MicroAnalysis Laboratory, Canada) with an acceleration voltage of 10 kV, a beam current of 10 nA and a beam diameter of 5 μm. The following reference materials were used: cuprite (Cu*Lα*) and tugtupite (Cl*Kα*). The intensity data were corrected for Time Dependent Intensity (TDI) loss (or gain) using a self-calibrated correction for Cl*Kα*.

The Fourier-transform infrared spectrum of bounahasite was obtained at the Canadian Conservation Institute, Canada using a Bruker Hyperion 2000 microscope interfaced to a Tensor 27 spectrometer with a wide-band mercury cadmium telluride (MCT) detector. A crystal of bounahasite ~20 μm in size was mounted on a low-pressure diamond anvil microsample cell and analysed in transmission mode. The spectrum was collected between 400–4000 cm^{-1} with the co-addition of 150 scans at a 4 cm^{-1} resolution.

Powder X-ray diffraction data were collected at the Canadian Museum of Nature, Canada using a Bruker D8 Discover microdiffractometer equipped with a DECTRIS EIGER2 R 500K detector and IμS microfocus X-ray source ($\lambda CuK\alpha_1$ = 1.54060Å) with the $K\alpha_2$ contribution removed using the 'Strip Kα2' tool in Bruker Diffrac.EVA V4.3. The instrument was calibrated using a statistical calibration method (Rowe, 2009). A powder ball 200 μm in diameter, mounted on a fibre pin mount, was analysed with continuous Phi rotation and 10° rocking motion along the Psi axis of the Centric Eulerian Cradle stage.

Single-crystal X-ray studies were carried out at room temperature on a Rigaku XtaLAB Synergy-S diffractometer equipped with a HyPix 6000HE detector ($\lambda CuK\alpha$ = 1.54184) operating at 50 kV and 1 mA, housed at the Natural History Museum, University of Oslo, Norway. The data were collected and processed using Rigaku's *CrysAlis Pro* software.

Table 1. Chemical data (in wt.%, average of 3 analyses) for bounahasite.

Constituent	Mean	Range	S.D. (2σ)
[Cu_2O(total)]	69.78	69.20–70.63	0.75
CuO*	51.72		
Cu_2O*	23.26		
Cl	23.36	22.70–24.24	0.79
H_2O*	8.71		
$-O = Cl_2$	−5.27		
Total	101.78		

*Calculated from the stoichiometry.
S.D. – standard deviation

Results

Chemical data

Chemical data for bounahasite are given in Table 1. Obtaining good data proved to be very challenging due to the small size of the crystals, especially their thickness. We were able to collect only a few reliable analyses. The empirical formula calculated on the basis of 3 Cu atoms per formula unit is: $Cu^{+}Cu^{2+}_{2}(OH)_{2.97}Cl_{2.03}$. The content of Zn is below the detection limit. The ideal formula for bounahasite is $Cu^{+}Cu^{2+}_{2}(OH)_3Cl_2$, which requires Cu_2O 22.90, CuO 50.90, H_2O 8.64, Cl 22.68, $-O = Cl_2$ −5.12, total 100 wt.%.

Bounahasite is readily soluble in acids at room temperature.

Infrared spectroscopy

The infrared (IR) spectrum of bounahasite (Fig. 3) shows IR bands of O–H-stretching (in the range from 3470 to 3350 cm^{-1}) vibrations of OH groups and absorbed H_2O molecules (the wider band at 3350 cm^{-1}), as well as multiple bands in the range 400–1150 cm^{-1}. A weak broad band at 1630 cm^{-1} could be assigned to H–O–H bending vibrations of absorbed H_2O molecules. Similar weak bands are often observed in the IR spectra of copper(II) hydroxychloride minerals of the atacamite group (Chukanov, 2014). The latter are also characterised by multiple IR bands in the 400–600 and 750–1150 cm^{-1} ranges but the lack of bands in the range 600–750 cm^{-1}, unlike the spectrum of bounahasite with its distinct band at 684 cm^{-1}. Direct attribution of the bands in the range 400–1150 cm^{-1} is very challenging due to the paucity of compounds with comparable chemistry, and thus the lack of theoretical works on vibrations in them.

X-ray diffraction data

The indexed powder X-ray diffraction data are given in Table 2. Parameters of the monoclinic unit cell refined from the

https://doi.org/10.1180/mgm.2022.133 Published online by Cambridge University Press

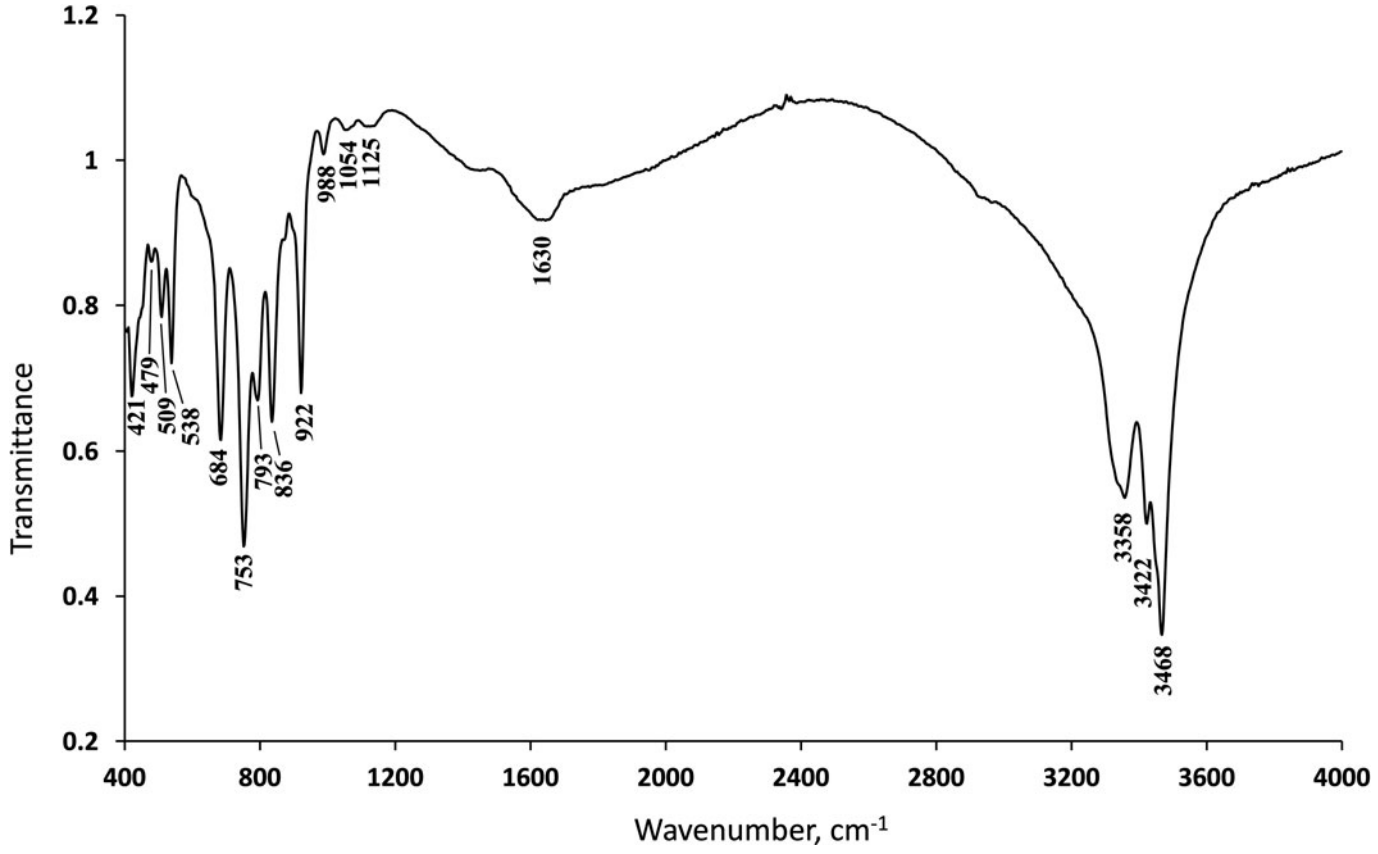

Fig. 3. Infrared spectrum of bounahasite

powder data are as follows: $a = 8.5906(2)$ Å, $b = 6.4203(1)$ Å, $c = 10.406(1)$ Å, $\beta = 111.783(1)°$ and $V = 532.98(2)$ Å^3.

The single-crystal X-ray diffraction data were indexed in the $P2_1/n$ space group with the following unit-cell parameters: $a = 8.5925(1)$, $b = 6.4189(1)$, $c = 10.4118(2)$ Å, $\beta = 111.804(2)°$ and $V = 533.17(2)$ Å^3. The structure was solved and refined to $R1 = 0.028$ on the basis of 1054 independent reflections with $I > 2\sigma(I)$ using the *SHELXL-2018/3* program package (Sheldrick, 2015). Crystal data, data collection and structure refinement details are given in Table 3, atom coordinates, equivalent displacement parameters, site occupancy factors in Table 4, selected interatomic distances in Table 5 and bond valence sums (BVS) in Table 6. The crystallographic information file has been deposited with the Principal Editor of *Mineralogical Magazine* and is available as Supplementary material (see below). In addition, it has been deposited in the Inorganic Crystal Structure Database (ICSD; #CSD 2189172).

Description and discussion of the crystal structure

The crystal structure of bounahasite is unique. It is based on two alternating sheets – octahedral and tetrahedral – coplanar to (110) (Fig. 4a,b). The octahedral sheet consists of alternating edge-sharing slightly Jahn–Teller-distorted $Cu(2)^{2+}(OH)_6$ octahedra with a <Cu–O> distance of 2.133 and two octahedra coordinated by oxygen and chlorine: $Cu(1)^{2+}(OH)_4Cl_2$ and $Cu(3)^{2+}(OH)_4Cl_2$. Both Cu(1)- and Cu(3)-centred octahedra are strongly distorted with short equatorial Cu–O bonds with <Cu–O> distances of 1.960 and 1.974 Å, respectively, and elongated axial Cu–Cl bonds (Fig. 5a; Table 5). The distortion is attributed to the pseudo Jahn–Teller effect observed in Cu^{2+}-centred octahedra with mixed ligands (Hathaway, 1984). Ignoring the long Cu–Cl bonds, the sheet can be described as consisting of alternating edge-sharing $Cu^{2+}(OH)_6$ octahedra and two $Cu^{2+}(OH)_4$ squares.

A similar sheet formed by alternating edge-sharing $Cu(OH)_4Cl_2$ and $Cu(OH)_5Cl$ octahedra was found in the structure of botallackite, $Cu_2(OH)_3Cl$ (Fig. 5b; Hawthorne, 1985).

The tetrahedral sheet is based on $Cu(4)^{+}Cl_4$ tetrahedra (Fig. 6). Two edge-sharing $Cu^{+}Cl_4$ tetrahedra form $Cu_2^{+}Cl_6$ dimers connected with each other via shared vertices (Fig. 7). The Cu4 site is split onto the Cu4a and Cu4b subsites (Fig. 8) with the occupancy factors 0.9596(17) and 0.0404(17) and <Cu–Cl> distances of 2.364 and 2.449 Å, respectively. The Cu4a–Cu4b distance is 1.24 Å. There are several peaks and holes in the electron density map between the Cu4a and Cu4b sites, which indicates further splitting with multiple low-occupancy Cu4 subsites located near the Cu4a site.

The two sheets are connected via Cl1 atoms. The weak bonding between the sheets explains the perfect cleavage in one direction and the platy habit of bounahasite.

Structural analysis was crucial in determining both the number and the nature of the anions in the formula, as well as the valence state of copper. The bond-valence sums (BVS) at the O1 [1.23 valence units (vu)], O2 [1.26 vu], and O3 [1.29 vu; Table 6] sites indicate that all three sites are occupied by hydroxyl groups. H atoms were tentatively localised in the structure (Fig. 4b, Table 7). The distances between H and

https://doi.org/10.1180/mgm.2022.133 Published online by Cambridge University Press

Table 2. Powder X-ray diffraction data of bounahasite.

I_{obs}	I^1_{calc}	d_{obs}	d^2_{calc}	*hkl*
70	**51**	**7.71**	**7.716**	**$\bar{1}$01**
22	**17**	**5.34**	**5.348**	**011**
13	11	4.998	5.002	110
11	9	4.068	4.072	111
100	**9, 100**	**3.856**	**3.861, 3.858**	**012, $\bar{2}$02**
2	3	3.471	3.467	$\bar{1}$03
5	5	3.387	3.388	210
10	8	3.210	3.210	020
3	3	3.046	3.050	$\bar{1}$13
14	3, 10	2.963	2.978, 2.964	120, $\bar{1}$21
9	6	2.847	2.848	$\bar{3}$01
7	3	2.820	2.820	$\bar{2}$13
15	15	2.740	2.741	121
5	6	2.708	2.708	$\bar{1}$22
36	**31**	**2.673**	**2.674**	**022**
30	**18**	**2.665**	**2.663**	**103**
6	4, 2	2.634	2.633, 2.604	202, $\bar{3}$11
5	3, 5	2.522	2.522, 2.501	$\bar{2}$04, 220
6	4	2.458	2.457	310
3	3	2.406	2.406	$\bar{1}$14
71	**46, 38, 3**	**2.350**	**2.355, 2.350, 2.348**	**$\bar{1}$23,301, $\bar{2}$14**
17	18	2.130	2.131	$\bar{3}$21
17	16	2.062	2.062	$\bar{1}$05
14	2, 12, 4	1.9835	1.9943, 1.9834, 1.9827	400, $\bar{2}$24, 131
12	13	1.9296	1.9291	$\bar{4}$04
5	4	1.8210	1.8211	$\bar{1}$33
6	5	1.7842	1.7838	$\bar{4}$22
4	2	1.7550	1.7544	411
4	2	1.7353	1.7347	$\bar{1}$25
7	8	1.6776	1.6773	$\bar{5}$01
8	8, 2	1.6630	1.6626, 1.6535	$\bar{3}$25, $\bar{4}$24
4	4	1.6053	1.6051	040
6	8	1.5719	1.5714	$\bar{1}$41
17	14	1.5653	1.5651	224
4	4	1.5401	1.5403	323
3	3	1.5279	1.5275	125
3	4	1.5049	1.5044	$\bar{5}$23

The strongest lines are given in bold.
[1]Calculated from the crystal structure determination, only reflections with intensities >1 are given.
[2]Calculated from powder XRD Rietveld unit-cell refinement with a = 8.5906(2), b = 6.4203(1), c = 10.406(1) Å, β = 111.783(1)° and V = 532.98(2) Å^3.

Table 3. Crystal data, data collection information and structure refinement details for bounahasite.

Crystal data	
Ideal formula	$Cu^+Cu^{2+}_2(OH)_3Cl_2$
Crystal dimensions (mm)	0.009 × 0.022 × 0.025
Crystal system, space group	Monoclinic, $P2_1/n$
a (Å)	8.5925(1)
b (Å)	6.4189(1)
c (Å)	10.4118(2)
β (°)	111.804(2)
V (Å^3)	533.17(2)
Z	4
Calculated density (g cm^{-3})	3.90
Absorption correction (mm^{-1})	22.28
Data collection	
Crystal description	Green pseudo-hexagonal plate
Instrument	Rigaku XtaLAB Synergy-S
Radiation type, wavelength (Å)	Cu$K\alpha$, 1.54184
Number of frames	10383
θ range (°)	5.73–79.81
Absorption correction	*CrysAlis Pro* (2019, Rigaku Oxford Diffraction)
T_{min}, T_{max}	0.816, 0.965
No. of measured, independent and observed [$I > 2\sigma(I)$] reflections	10591, 1146, 1054
R_{int}	0.033
Data completeness to 71.98°θ (%)	100
Indices range of h, k, l	$-10 \le h \le 10$, $-7 \le k \le 8$, $-13 \le l \le 13$
Refinement	
Refinement	Full-matrix least squares on F^2
Number of reflections, parameters, restraints	1146, 90, 3
R_1 [$I > 2\ \sigma I$], R_1(all)	0.028, 0.030
wR_2 [$I > 2\ \sigma I$], wR_2(all)	0.080, 0.083
GoF	1.02
No. of refined parameters	90
$\Delta\rho_{max}$ /$\Delta\rho_{min}$ (e^- Å^{-3})	0.77 / −1.18*

*Located 0.64 Å away from the Cu4a site.

O atoms were restrained during refinement using a soft restraint (0.85 Å using the DFIX command). Hydrogen bonding between O atoms of the octahedral sheet and Cl2 atoms of the tetrahedral sheet (O–H···Cl) connects the sheets. Each Cl2 atom is involved in three hydrogen bonds (Table 7). The low BVS at the Cl2 site [0.53 vu; Table 6] is due to the unaccounted hydrogen bonds contribution.

The BVS at the Cu1, Cu2 and Cu3 sites [2.16, 1.96 and 2.10 vu, respectively; Table 6] confirm the bivalent state of copper at those sites. Although, as discussed above, the splitting of the Cu4 site

Table 4. Coordinates, equivalent (U_{eq}) and anisotropic displacement parameters (in Å^2) of atoms, and site-occupancy factors[#] for bounahasite.

Site	Wyck	*x/a*	*y/b*	*z/c*	U_{eq}	U^{11}	U^{22}	U^{33}	U^{23}	U^{13}	U^{12}
Cu1	2d	1	½	½	0.0124(2)	0.0152(4)	0.0084(3)	0.0102(3)	0.0008(2)	0.0010(3)	0.0000(2)
Cu2	2b	½	½	0	0.0134(2)	0.0130(4)	0.0096(4)	0.0115(4)	−0.0018(2)	−0.0023(3)	0.0007(2)
Cu3	4e	0.75010(5)	0.73045(8)	0.24720(4)	0.01346(18)	0.0121(3)	0.0118(3)	0.0115(3)	−0.00103(14)	−0.0014(2)	0.00040(15)
Cu4a[#]	4e	0.36367(8)	0.40488(12)	0.36040(7)	0.0389(2)*	0.0311(4)	0.0497(5)	0.0327(4)	−0.0055(3)	0.0082(3)	−0.0018(3)
Cu4b[#]	4e	0.3683(18)	0.598(3)	0.3677(15)	0.0389(2)*	0.0311(4)	0.0497(5)	0.0327(4)	−0.0055(3)	0.0082(3)	−0.0018(3)
Cl1	4e	0.65355(9)	0.49064(11)	0.42340(7)	0.0186(2)	0.0168(4)	0.0222(4)	0.0172(4)	−0.0022(2)	0.0070(3)	−0.0017(3)
Cl2	4e	0.17127(12)	0.53849(15)	0.16106(9)	0.0309(2)	0.0325(5)	0.0335(5)	0.0255(4)	0.0005(3)	0.0095(4)	0.0057(4)
O1	4e	0.9833(3)	0.7026(4)	0.3608(2)	0.0145(4)	0.0133(10)	0.0147(10)	0.0137(10)	0.0033(8)	0.0029(8)	0.0005(8)
H1	4e	1.027(7)	0.662(9)	0.314(5)	0.047(15)						
O2	4e	0.7399(3)	0.4778(3)	0.1322(2)	0.0143(5)	0.0141(11)	0.0137(10)	0.0126(11)	0.0017(7)	0.0020(9)	0.0000(8)
H2	4e	0.808(6)	0.476(9)	0.093(5)	0.05**						
O3	4e	0.5143(3)	0.7508(3)	0.1203(2)	0.0142(4)	0.0139(10)	0.0155(10)	0.0118(10)	0.0008(8)	0.0030(8)	0.0006(8)
H3	4e	0.468(7)	0.751(8)	0.168(5)	0.05**						

Site-occupancy factor for Cu4a is $Cu_{0.9596(17)}$ and Cu4b is $Cu_{0.0404(17)}$, all other sites = 1
*The anisotropic displacement parameters for Cu4a and Cu4b were refined constraining site movements and occupancies to each other (the EADP command).
**U_{iso}; the values were fixed during refinement.

https://doi.org/10.1180/mgm.2022.133 Published online by Cambridge University Press

Table 5. Selected interatomic distances (Å) in the structure of bounahasite.

Cu1–O1	1.913(2) ×2	Cu4a–Cl2	2.2863(11)
Cu1–O3	2.007(2) ×2	Cu4a–Cl2	2.3710(13)
Cu1–Cl1	2.7817(7) ×2	Cu4a–Cl1	2.3924(9)
<Cu1–O>	1.960	Cu4a–Cl1	2.4054(9)
		<Cu4a–Cl>	2.364
Cu2–O2	2.014(2) ×2		
Cu2–O3	2.016(2) ×2	Cu4b–Cl2	2.222(15)
Cu2–O1	2.368(2) ×2	Cu4b–Cl1	2.323(15)
<Cu2–O>	2.133	Cu4b–Cl1	2.401(15)
		Cu4b–Cl2	2.850(18)
Cu3–O1	1.920(2)	<Cu4b–Cl>	2.449
Cu3–O3	1.970(2)		
Cu3–O2	1.999(2)	O1–H1	0.76(5)
Cu3–O2	2.006(2)	O2–H2	0.83(4)
Cu3–Cl1	2.7485(8)	O3–H3	0.74(4)
Cu3–Cl1	2.7789(8)		
<Cu3–O>	1.974		

Table 6. Bond-valence calculations* for bounahasite.

	Cu1	Cu2	Cu3	Cu4a	Σ
Cl1	$0.12^{\times 2\downarrow}$		0.13	0.22	0.80
			0.12	0.21	
Cl2				0.30	0.53
				0.23	
O1	$0.54^{\times 2\downarrow}$	$0.16^{\times 2\downarrow}$	0.53		1.23
O2		$0.41^{\times 2\downarrow}$	0.43		1.26
			0.42		
O3	$0.42^{\times 2\downarrow}$	$0.41^{\times 2\downarrow}$	0.47		1.30
Σ	2.16	1.96	2.10	0.96	

*Bond-valence parameters were taken from Gagné and Hawthorne (2015) for Cu^{2+}–O bonds and Brese and O'Keeffe (1991) for Cu^{2+}–Cl and Cu^{+}–Cl bonds.

into multiple subsites complicates bond-valence calculations for both Cu and Cl sites, the results are unambiguous. The BVS calculated using bond-valence parameters taken for Cu^{2+}–Cl bonds (Brese and O'Keeffe, 1991) is 1.44 vu, whereas the parameters were taken for Cu^{+}–Cl bonds give 0.96 vu, indicating that Cu^{+} is the dominant valence state of copper at the Cu4 site.

The resulting structural formula of bounahasite is $Cu^{+}Cu_2^{2+}Cl_2(OH)_3$.

No minerals or synthetic compounds structurally related to bounahasite have been found in the literature or databases. All five copper hydroxychlorides that have been found in Nature so far (atacamite $Cu_2Cl(OH)_3$, belloite Cu(OH)Cl, botallackite $Cu_2Cl(OH)_3$, clinoatacamite $Cu_2Cl(OH)_3$ and paratacamite $Cu_3(Cu,Zn)Cl_2(OH)_6$ [IMA-CNMNC List of Mineral Names, Pasero, 2022] contain only bivalent copper, and their structures are based on Cu-centred polyhedra with mixed Cl^- and OH^- ligands (Wells, 1949; Fleet, 1975; Hawthorne, 1985; Grice *et al.*, 1996; Pollard *et al.*, 1989; Krivovichev *et al.*, 2017; Zheng *et al.*, 2018).

It is rare to find Cu–Cl polyhedra in minerals and occurrences are usually structural types unique to each mineral, for example vertex-sharing $Cu^{+}Cl_4$ tetrahedra in nantokite CuCl, which is a representative of the sphalerite structural type (Wyckoff and Posnjak, 1922), distorted octahedra $Cu^{2+}Cl_6$ in tolbachite $CuCl_2$ (Burns and Hawthorne, 1993) or discrete planar dimers $Cu_2^{2+}Cl_6$ in sanguite $KCuCl_3$ (Pekov *et al.*, 2015). In this study, the tetrahedral sheet of bounahasite is no exception, as no sheet of a similar topology has been described before in either minerals or synthetic compounds. This implies that there is no preferential stable configuration of Cu–Cl polyhedra. All three minerals mentioned above – nantokite, tolbachite and sanguite – are unstable in air and alter into secondary minerals. Bounahasite has shown no signs of alteration so far, possibly due to the octahedral sheet stabilising the structure. The splitting of the Cu4 site into multiple subsites may play a similar role by relaxing the bonds and thus satisfying the local charge balance within the tetrahedral sheet.

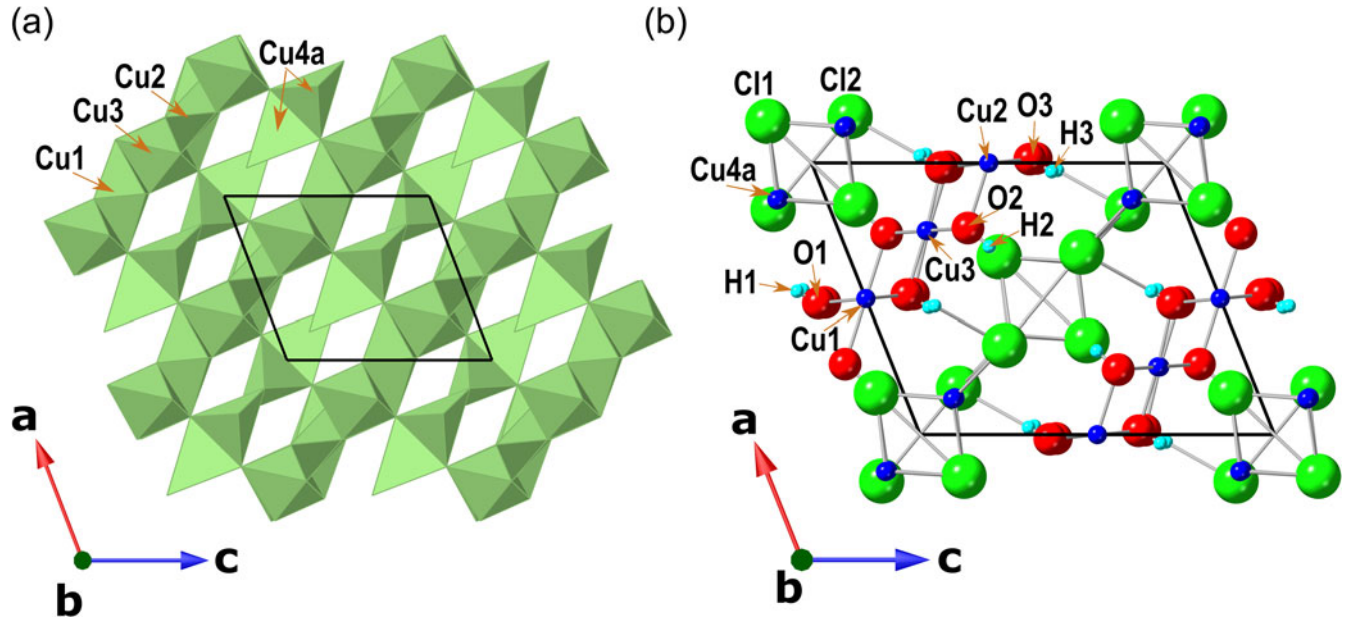

Fig. 4. General view of the crystal structure of bounahasite: (a) polyhedral and (b) ball-and-stick models. The unit cell is outlined. Projection on (001).

https://doi.org/10.1180/mgm.2022.133 Published online by Cambridge University Press

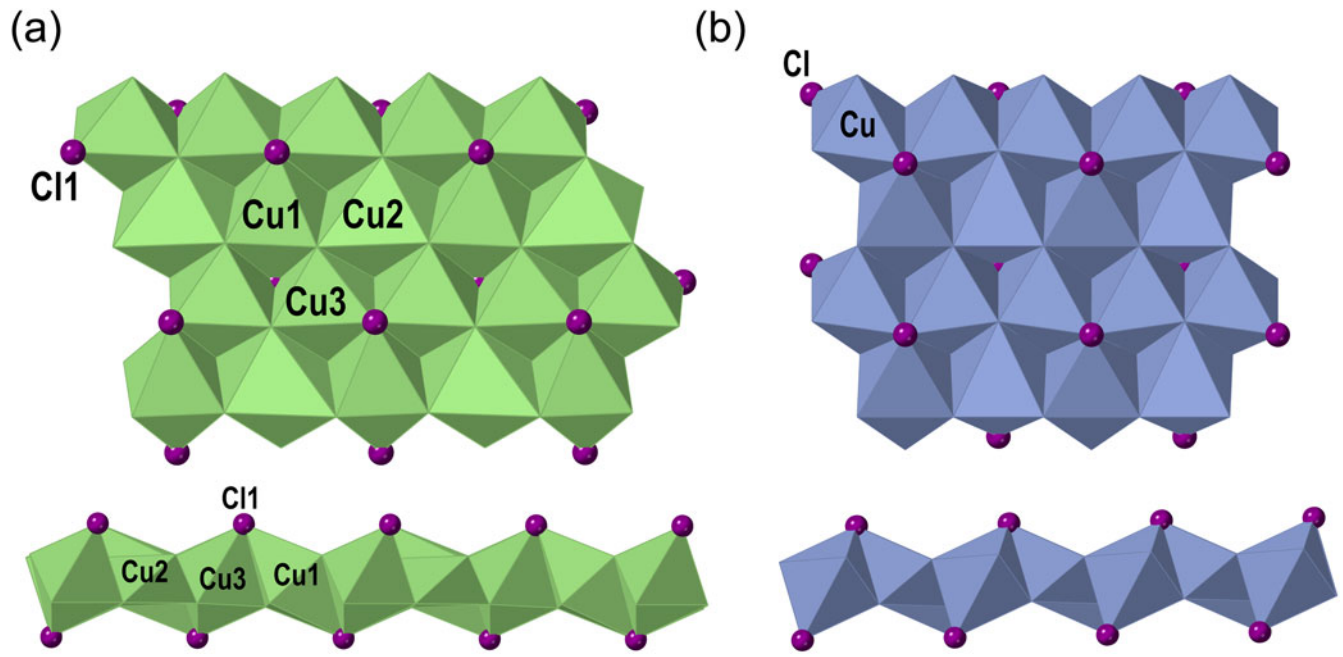

Fig. 5. (a) Octahedral sheet in the crystal structure of bounahasite and (b) a similar sheet in the crystal structure of botallackite (after Hawthorne, 1985).

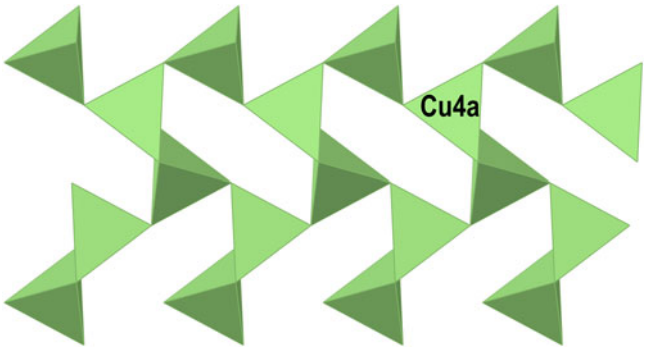

Fig. 6. Tetrahedral sheet in the crystal structure of bounahasite.

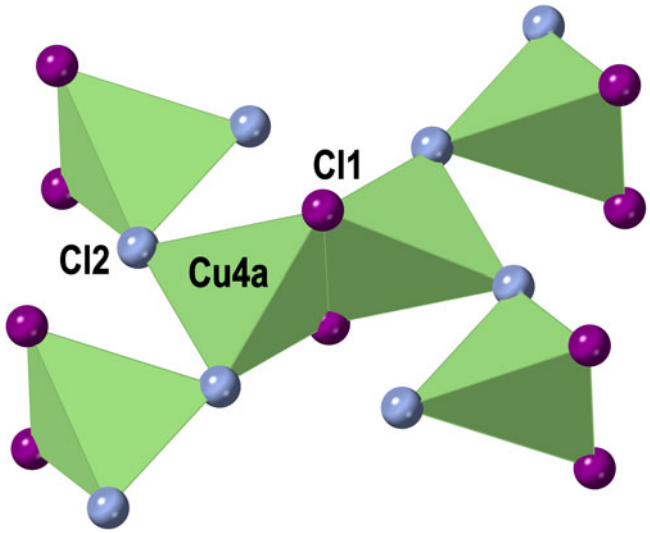

Fig. 7. $Cu_2^{2+}Cl_6$ dimer connected with other dimers via shared vertices in the crystal structure of bounahasite.

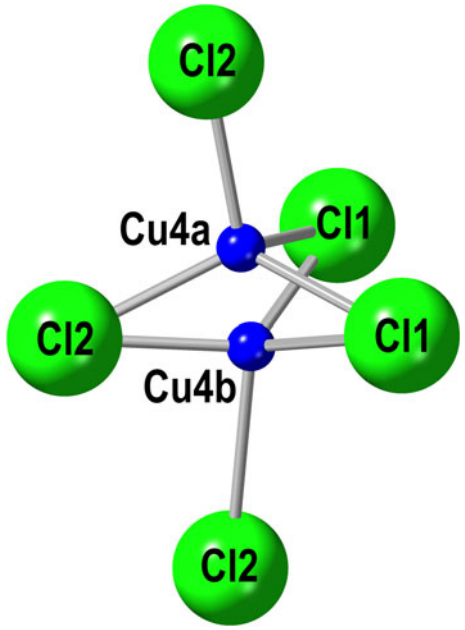

Fig. 8. Splitting of the Cu4 site into two subsites in the crystal structure of bounahasite.

Table 7. Hydrogen bonds in the structure of bounahasite.*

D–H···*A*	*d*(*D*–H), Å	*d*(H···*A*), Å	∠(*D*–H···*A*), °	*d*(*D*···A), Å
O1–H1···Cl2	0.76(5)	2.49(5)	178(6)	3.247(2)
O2–H2···Cl2	0.83(4)	2.72(5)	142(5)	3.413(2)
O3–H3···Cl2	0.74(4)	2.87(5)	133(5)	3.413(2)

**D* = donor; *A* = acceptor

https://doi.org/10.1180/mgm.2022.133 Published online by Cambridge University Press

Acknowledgements. We thank anonymous referees for their valuable comments. We thank Donald Doell Jr. for donating a suite of specimens, one of which became the holotype of bounahasite, to the Canadian Museum of Nature. We are grateful to François Génier for taking the colour photo.

Supplementary material. To view supplementary material for this article, please visit https://doi.org/10.1180/mgm.2022.133

Competing interests. The authors declare none.

References

Brese N.E. and O`Keeffe M. (1991) Bond-valence parameters for solids. *Acta Crystallographica,* **B47**, 192–197.

Burns P.C. and Hawthorne F.C. (1993) Tolbachite, $CuCl_2$, the first example of Cu^{2+} octahedrally coordinated by Cl^-. *American Mineralogist*, **78**, 187–189.

Chukanov N.V. (2014) *Infrared Spectra of Mineral Species*. Springer, Dordrecht. 1726 pp.

Fleet M. (1975) The crystal structure of paratacamite, $Cu_2(OH)_3Cl$. *Acta Crystallographica,* **B31**, 183–187.

Gagné O.C. and Hawthorne F.C. (2015) Comprehensive derivation of bond-valence parameters for ion pairs involving oxygen. *Acta Crystallographica,* **B71**, 562–578.

Grice J.D., Szymanski J.T. and Jambor J.L. (1996) The crystal structure of clinoatacamite, a new polymorph of $Cu_2(OH)_3Cl$. *The Canadian Mineralogist*, **34**, 73–78.

Hathaway B.J. (1984) A new look at the stereochemistry and electronic properties of complexes of the copper(ii) ion. Pp. 55–118. in: *Complex Chemistry*. Conference Proceedings, Springer, Berlin.

Hawthorne F.C. (1985) Refinement of the crystal structure of botallackite. *Mineralogical Magazine*, **49**, 87–89.

Krivovichev S.V., Filatov S.K., Burns P.C. and Vergasova L.P. (2006) The crystal structure of allochalcoselite, $Cu^+Cu_5^{2+}PbO_2(SeO_3)_2Cl_5$, a mineral with well-defined Cu^+ and Cu^{2+} positions. *The Canadian Mineralogist*, **44**, 507–514.

Krivovichev S.V., Hawthorne F.C. and Williams P.A. (2017) Structural complexity and crystallization: The ostwald sequence of phases in the $Cu_2(OH)_3Cl$ system (botallackite–atacamite–clinoatacamite). *Structural Chemistry*, **28**, 153–159.

Lykova I., Rowe R., Poirier G., Friis H. and Helwig K. (2022) Bounahasite, IMA 2021-114. CNMNC Newsletter 67. *Mineralogical Magazine*, **86**, 849–853.

Mandarino J.A. (1981) The gladstone-dale relationship; part IV, the compatibility concept and its application. *The Canadian Mineralogist*, **19**, 441–450.

O'Keeffe M. and Bovin J.-O. (1978) The crystal structure of paramelaconite, Cu_4O_3. *American Mineralogist*, **63**, 180–185.

Pasero M. (2022) *The New IMA List of Minerals*. International Mineralogical Association. Commission on new minerals, nomenclature and classification (IMA-CNMNC). http://cnmnc.main.jp/ [Accessed 09 July 2022].

Pekov I.V., Zubkova N.V., Belakovskiy D.I., Lykova I., Yapaskurt V.O., Vigasina M.F., Sidorov E.G. and Pushcharovsky D.Y. (2015) Sanguite, $KCuCl_3$, a new mineral from the Tolbachik volcano, Kamchatka, Russia. *The Canadian Mineralogist*, **53**, 633–641.

Pollard A.M., Thomas R.G. and Williams P.A. (1989) Synthesis and stabilities of the basic copper(II) chlorides atacamite, paratacamite and botallackite. *Mineralogical Magazine*, **53**, 557–563.

Praszkier T. (2015) Neufunde von gediegenem Kupfer in Kristallen aus Bou N'has, Oumjrane, Marokko. *Mineralien-Welt,* **5**/2015, 62–71.

Rowe R. (2009) New statistical calibration approach for Bruker AXS D8 Discover microdiffractometer with Hi-Star detector using GADDS software. *Powder Diffraction*, **24**, 263–271.

Sheldrick G.M. (2015) Crystal structure refinement with SHELXL. *Acta Crystallographica,* **C71**, 3–8.

Vergasova L.P., Krivovichev S.V., Britvin S.N., Filatov S.K., Burns P.C., and Ananyev V.V. (2005) Allochalcoselite, $Cu^+Cu_5^{2+}PbO_2(SeO_3)_2Cl_5$ - a new mineral from volcanic exhalations (Kamchatka, Russia). *Zapiski Rossiiskogo Mineralogicheskogo Obshchetstva*, **134**, 70–74 [in Russian].

Wells A. (1949) The crystal structure of atacamite and the crystal chemistry of cupric compounds. *Acta Crystallographica*, **2**, 175–180.

Wyckoff R.W.G. and Posnjak E. (1922) The crystal structures of the cuprous halides. *Journal of the American Chemical Society*, **44**, 30–36.

Zheng X.-G., Yamauchi I., Kitajima S., Fujihala M., Maki M., Lee S., Hagihala M., Torii S., Kamiyama T. and Kawae T. (2018) Two-dimensional triangular-lattice Cu(OH)Cl, belloite, as a magnetodielectric system. *Physical Review Materials*, **2**, 104401.